Chapter 4

Plectonemes?

> Generally, things obtained without exertion
> are not that useful.
>
> Giuseppe de Marco

In the previous chapter we have mainly investigated the interaction between DNA molecules and nucleosomes. However also naked DNA behaves in an interesting fashion. Take, for example, the DNA persistence length, $l_p \approx 50\,\text{nm}$: it was found by measuring the extension of the molecule when stretched with different forces.

However when the molecule is also twisted, various theories were proposed, but a unifying framework to describe the experimental results was lacking. This is partly due to the important role of thermal fluctuations, extensively analyzed for low torques [51], but either left out [5, 49, 8] or partially added by hand for high torques [50].

In section 1.5, the *bifurcation point* of a straight rod (that is without writhe, see section 1.3 in the same chapter) was identified. In terms of the number of inserted turns, the bifurcation point is at $n_{\text{crit}} = \sqrt{Af}L_c/\pi C$ where L_c is the contour length of the DNA, f the force applied to it, and A and C are related to the bending and torsional persistence lengths (see subsection 1.1) by $A = k_B T l_p$, $C = k_B T l_t$.

Since the DNA molecule is self-avoiding, the cheapest way to produce writhe is the *plectoneme*, a stretch of the chain branching off in a

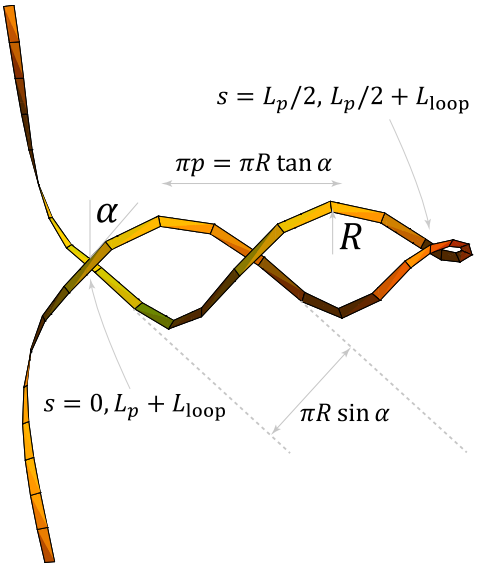

Figure 4.1: A plectoneme, along with the end loop, closing it, and the rest of the straight DNA. The path describing the plectoneme is parametrized by s, going from 0 to $L_p/2$ and from $L_p/2 + L_{\text{loop}}$ to $L_p + L_{\text{loop}}$. The gap is filled by the end loop.

perpendicular direction from the remaining two tails. The two halves circle around each other in a helical path like an old fashioned telephone wire and are connected by an *end loop* (see figure 4.1). A system with a sufficient number of turns n inserted has a plectoneme (plus the tails) as its ground state. This transition typically happens before n_{crit}. Since the molecule is too small to directly observe plectoneme formation, their presence is inferred by measuring the DNA end-to-end extension as a function of n. These curves are called the *turn-extension curves* and the increase in plectoneme length L_p is observed as a linear decrease of the end-to-end extension after the transition.

4.1 The DNA shape

For the shape of the molecule, as seen in figure 4.1, we assume that the tails are given by the homoclinic solutions (eqs. (1.31–1.32)) for $t > t_c \approx 0.80424$. We restrict t since we "attach" the plectoneme at the non-zero point of closest approach of the two tails, which exists only when $t > t_c$. At the point of closest approach the distance between the two tails can be approximated by

$$d_{\text{crit}}(t) = 2\lambda\left(\sqrt{\frac{1-t}{0.3799}} - 0.00112\right). \tag{4.1}$$

Therefore the radius of the plectoneme is given by $R(t) = d_{\text{crit}}(t)/2$. Its path, on the other hand, can be parametrized by

$$\mathbf{r}_p = \begin{pmatrix} (s_0 + s)\sin\alpha \\ -R(t)\cos\left((s_0+s)\frac{\cos\alpha}{R(t)}\right) \\ R(t)\sin\left((s_0+s)\frac{\cos\alpha}{R(t)}\right) \end{pmatrix} \quad \text{for} \quad s \in [0, L_p/2]$$
$$\mathbf{r}_p = \begin{pmatrix} (s_0 + L_p + L_{\text{loop}} - s)\sin\alpha \\ R(t)\cos\left((s_0+L_p+L_{\text{loop}}-s)\frac{\cos\alpha}{R(t)}\right) \\ -R(t)\sin\left((s_0+L_p+L_{\text{loop}}-s)\frac{\cos\alpha}{R(t)}\right) \end{pmatrix} \quad \text{for} \quad s \in [0, L_p/2], \tag{4.2}$$

where α is plectoneme angle (see fig. 4.1) and L_p, L_{loop} are the contour lengths of the plectoneme and of the loop. The starting orientation depends on the homoclinic solution and is set by s_0, chosen so that the tails are attached in a continuous fashion to the plectoneme.

4.2 The writhe

We can first calculate the writhe of the plectoneme by using the tangent of eq (4.2) and the $\hat{x}$-axis in eq. (1.39):

$$\begin{aligned}\omega_1(s) &= \frac{1}{2\pi}\frac{\cos\alpha(\sin\alpha-1)}{R(t)} \quad s\in[0,l_p/2],\\ \omega_2(s) &= \frac{1}{2\pi}\frac{\cos\alpha(\sin\alpha+1)}{R(t)} \quad s\in[l_p/2+l_l,l_p+l_l].\end{aligned} \tag{4.3}$$

This expression neglects end loop and tails; by summing ω_1 and ω_2 one arrives at an "average" writhe density

$$\omega^0(\alpha,t) = \frac{\cos\alpha\sin\alpha}{2\pi R(t)}. \tag{4.4}$$

This expression is very convenient, and it was normally taken to be the writhe density of the plectoneme [49]. However, when we computed the writhe of the tails in eq. (1.35), the reference axis was the $\hat{z}$-axis, parallel to the force F, and not the $\hat{x}$-axis as in the case of eqs. (4.3). To be consistent (the non-locality of the writhe forbids, in fact, to use different reference axes in Fuller formula, eq. (1.39), for different sections of the curve) we compute the writhe of the plectoneme with respect to the $\hat{z}$-axis, resulting in

$$\begin{aligned}\omega_b(s) = \frac{1}{2\pi}\frac{\sin\alpha\cos\alpha}{R(t)}\times\\ \times\left[1-\frac{1}{1+\cos\alpha\cos\left((s+s_0)\frac{\cos\alpha}{R(t)}\right)}\right].\end{aligned} \tag{4.5}$$

This expression is annoying as it is s-dependent. However, while the plectoneme grows, the writhe of the end loop changes, as it changes its orientation. This loop is described by a space curve $\mathbf{r}_0 = (r_x(u), r_y(u), r_z(u))$, $u\in[0,L_{\text{loop}}]$, subject to the conditions, at its boundaries, $\mathbf{r}_0(0) = \mathbf{r}_p(0)$ and $\mathbf{r}_0(L_{\text{loop}}) = \mathbf{r}_p(L_{\text{loop}})$. We also assume (unlike at the boundaries between tails and plectoneme) that the curve is smooth between plectoneme and end loop.

Increasing the contour length by an amount $2s$ causes a rotation of $\mathbf{r}_0$ by an angle $\xi(s) = s\cos\alpha/R(t)$ (see eq. (4.2)) about the $\hat{x}$-axis, inducing an s-dependent change in the writhe of the loop

$$\begin{aligned} Wr_{\text{loop}} =& \frac{1}{2\pi}\int_0^{L_{\text{loop}}} \mathrm{d}u \frac{\cos\xi(s)(t_x(u)\dot{t}_y(u) - \dot{t}_x(u)t_y(u)}{1-\sin\xi(s)t_y(u)+\cos\xi(s)t_z(u)} \\ & -\frac{1}{2\pi}\int_0^{L_{\text{loop}}} \mathrm{d}u \frac{\sin\xi(s)(t_z(u)\dot{t}_x(u) - \dot{t}_z(u)t_x(u)}{1-\sin\xi(s)t_y(u)+\cos\xi(s)t_z(u)}. \end{aligned} \tag{4.6}$$

A change in the plectoneme contour length induces a differential change of this writhe equal to

$$\begin{aligned} \frac{\mathrm{d}Wr_{\text{loop}}}{\mathrm{d}s} =& -\frac{\cos\alpha}{2\pi R(t)}\times \qquad (4.7) \\ & \left(\int_0^{l_l} \mathrm{d}u \frac{\dot{t}_x(u) + \sin\left(s\frac{\cos\alpha}{R(t)}\right)(t_x(u)\dot{t}_y(u) - \dot{t}_x(u)t_y(u))}{\left(1-\sin\left(s\frac{\cos\alpha}{R(t)}\right)t_y(u)+\cos\left(s\frac{\cos\alpha}{R(t)}\right)t_z(u)\right)^2} + \right. \\ & \left. \int_0^{l_l} \mathrm{d}u \frac{\cos\left(s\frac{\cos\alpha}{R(t)}\right)(t_z(u)\dot{t}_x(u) - \dot{t}_z(u)t_x(u))}{\left(1-\sin\left(s\frac{\cos\alpha}{R(t)}\right)t_y(u)+\cos\left(s\frac{\cos\alpha}{R(t)}\right)t_z(u)\right)^2}\right) \\ =& \frac{\cos\alpha}{\pi R(t)} \times \frac{t_x(0)}{1-\sin\left(s\frac{\cos\alpha}{R(t)}\right)t_y(0)+\cos\left(s\frac{\cos\alpha}{R(t)}\right)t_z(0)}, \qquad (4.8) \end{aligned}$$

where we used the unimodularity of the tangent vector and its symmetry: $t_x(0) = -t_x(L_{\text{loop}}), t_{y,z}(0) = t_{y,z}(L_{\text{loop}})$. Making use of the boundary conditions we finally find

$$\frac{\mathrm{d}Wr_{\text{loop}}}{\mathrm{d}s} = \frac{\cos\alpha\sin\alpha}{\pi R(t)}\left(1+\cos\alpha\cos\left((s_0+s)\frac{\cos\alpha}{R(t)}\right)\right)^{-1} \tag{4.9}$$

By adding this differential writhe density to the "bare" writhe density of the plectoneme ((4.5)) (half of it to each strand) we recover the standard writhe density of a plectoneme (4.4), but now with the added bonus that

the remaining writhe of the closing loop is independent of the length of the plectoneme. Since only in the end loop the antipodal points appear along the homotopy, defined by the explicit formation of the plectoneme, we can state that in this sense the writhe is additive:

$$Wr(t,\alpha) = Wr_{\text{loop}}(t) + L_p\omega^0(t,\alpha), \tag{4.10}$$

with Wr_{loop} and ω given by (1.35) and (4.4).

4.3 Mechanical and electrostatic energy

Starting point for the mechanical Hamiltonian of the system is eq. (1.49). Since the *number of turns* is experimentally controlled, we can write

$$H_M = \int_0^{L_c} \mathrm{d}s \left(\frac{A}{2}\dot{\mathbf{t}}_s^2 - \mathbf{f}\cdot\mathbf{t}_s \right) + 2\pi^2 \frac{C}{L_c}\left(n - Wr\right)^2 \tag{4.11}$$

where the writhe Wr is given by eq. (4.10). Using the bending energy of the homoclinic solution, eq. (1.33), and the plectoneme path eq. (4.2), we arrive at

$$E_M = -f(L_c - L_p) + E_{\text{loop}} + E^0_{\text{bend}} + 2\pi^2 \frac{C}{L}\left(n - Wr\right)^2 \tag{4.12}$$

$$E^0_{\text{bend}} = L_p \frac{A}{2}\frac{\cos^4\alpha}{R^2(t)}. \tag{4.13}$$

However, since many experiments are performed at low salt concentration, where the negatively charged DNA is less “screened”, electrostatic interactions change the energy. First the bending persistence length is renormalized according to the OSF theory [52, 63]:

$$l_p = l_p^{(0)} + \frac{\kappa^{-2}}{4Q_B} \tag{4.14}$$

where κ^{-1} is the Debye screening length and Q_B the Bjerrum length

$$Q_B = \frac{q^2}{4\pi\varepsilon_0\varepsilon_r k_B T} \tag{4.15}$$

$$\kappa = \sqrt{8\pi Q_B n_s} \tag{4.16}$$

where q is the elementary charge, ε_0 the vacuum permittivity, ε_r the dielectric constant and n_s the number density of the salt molecules. At $T = 300\,\mathrm{K}$, $Q_B \approx 0.715\,\mathrm{nm}$ and $\kappa = 0.1\sqrt{c_s}$, where c_s is the salt concentration in mM (milliMolar).

In the plectoneme there is another electrostatic effect: the two strands of DNA repeal each other, resulting in an energetic contribution [68]

$$E^0_{\mathrm{el}} = L_p \nu^2_{\mathrm{eff}} \frac{Q_B}{2} \sqrt{\frac{\pi}{\kappa R(t)}} e^{-2\kappa R(t)}\, \mathrm{Z}(\cot\alpha) \tag{4.17}$$

$$\mathrm{Z}(x) = 1 + 0.828x^2 + 0.868x^4$$

if $\cot\alpha < 1$, with ν_{eff} the effective charge density of the centerline of a charged cylinder source of a Debye-Hückel potential that asymptotically coincides in the small potential, far field, region with the non-linear Poisson-Boltzmann potential of that cylinder with a given surface charge (for DNA $2\,e/0.34$ nm, radius 1 nm).

To compute ν_{eff} and R^* as in figure 4.2 we follow [53]. The radius R^* marks the breaking down of the linearized theory, as there the reduced potential equals 1 [53]. The energy E_M changes therefore to

$$E^0 = E_M + E^0_{\mathrm{el}} \tag{4.18}$$

where the superscript indicates that no thermal fluctuations are taken into account up to now and where the persistence length should be taken as in eq. (4.14).

A plectoneme will form when the energy E^0 has a global minimum for $L_p > 0$. Minimization of the energy shows that this *transition point* happens at $n < n_{\mathrm{crit}}$. Moreover the angle α stabilizes between $\pi/2$, where $E_{\mathrm{bend}} = 0$, and $\pi/4$, where Wr is maximized and thus $n - Wr$ is minimized.

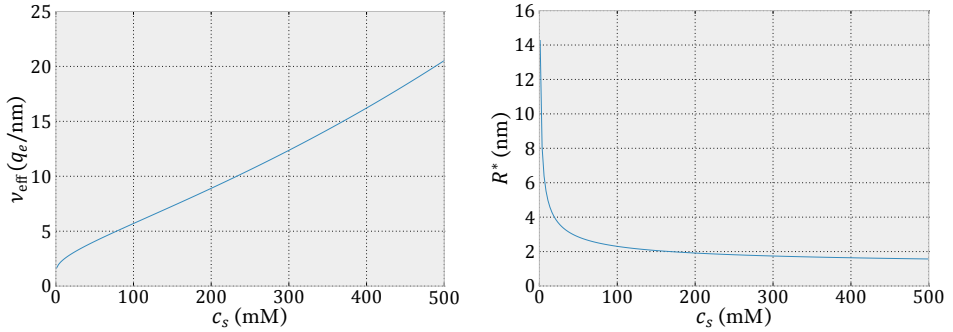

Figure 4.2: ν_{eff} and R^* as a function of the salt concentration c_s.

4.4 Fluctuations

The effect of thermal fluctuations is difficult to treat and complicated to analyze. Without entering in the details, we will explain the origin of each term, referring the reader to the specific papers for the details.

The first contribution from thermal fluctuations is the enhancement of the electrostatic interactions in the plectoneme. There the thermal undulations couple non-linearly with the electrostatic interactions [68]. As a result the interactions are strongly enhanced. In fact assuming the fluctuations to have a Gaussian distribution we can estimate their effect by considering one strand of the plectoneme in the mean field potential of the opposing strand. The undulations in the plectoneme are taken in two directions, along the radius and the pitch. The radial direction is limited by the exponent of E^0_{el} in eq. (4.17), $-2\kappa R(t)$, while in the pitch direction the limit is geometrical (see figure 4.1) so that we will assume that the standard deviation in that direction is fixed and equal to $\sigma_p = \pi R(t) \sin\alpha$. Calling σ_r the standard deviation in the radial direction, the electrostatic interaction becomes

$$E_{\text{el}} = E^0_{\text{el}} e^{4\kappa^2\sigma_r^2}. \tag{4.19}$$

The steep potential limits σ_r to $\approx \kappa^{-1}/2$. Here σ_p is not present as it only affects marginally the electrostatic energy [68]. Confining the DNA in the plectoneme has also an entropic cost. In fact the polymer has a

lower number of configurations as it is restricted in the radial direction by an harmonic potential, and in the pitch direction by a hard wall potential (represented by the consecutive turn of the strand). Burkhardt [6] computed the entropic contribution of such a confinement, but only for the torsion-less case. Recently Emanuel [20] worked out the more difficult case where torque is present. The result is that two deflection lengths appear, one for each confinement direction, $\lambda_{r,p} = (P_b \sigma^2_{r,p})^{1/3}$. The new effective deflection length for the plectoneme as a whole is then

$$\bar{\lambda} = 2\frac{\lambda_r^3\lambda_p + \lambda_r^2\lambda_p^2 + \lambda_r\lambda_p^3}{(\lambda_r + \lambda_p)(\lambda_r^2 + \lambda_p^2)} \tag{4.20}$$

which contributes to a confinement free energy equal to

$$E_C = \frac{3}{8}k_B T(\lambda_r^{-1} + \lambda_p^{-1})L_p. \tag{4.21}$$

Moreover fluctuations inside the plectoneme reduce its contour length by a factor [21]

$$\rho_{\mathrm{pl}} = 1 - \frac{k_B T}{4A}(\lambda_r + \lambda_p) \tag{4.22}$$

that in turn change the bending energy eq. (4.13) and the writhe density of the plectoneme eq. (4.4) to

$$E_{\mathrm{bend}} = E^0_{\mathrm{bend}}\rho^4_{\mathrm{pl}} \tag{4.23}$$

$$\omega(\alpha, t) = \omega^0(\alpha, t)\rho_{\mathrm{pl}}. \tag{4.24}$$

Outside the plectoneme, before the transition point, thermal fluctuations also play a role. In fact, the straight solution $\vartheta, \varphi = 0$ incurs in finite deformation $\mathrm{d}\vartheta, \mathrm{d}\varphi$ on top of it. These deformations, in general, alter the writhe of the chain. As a consequence, in a torsionally constrained setup, the White relation eq. (1.38) implies that the twist in influenced by fluctuations. In practice the torsional persistence length is rescaled to

$$C(\lambda) = \frac{C}{1 + \frac{Ck_BT}{4A\lambda f}} \tag{4.25}$$

where $\lambda = \sqrt{A/f}$ in this case. When computing the torsional energy we should use $C(\lambda)$ instead of C. However there is no reason the λ used in the tails should be reused in the plectoneme. The correct way to do it, in fact, is to use $\bar{\lambda}$ from eq. (4.20) for the torsional energy of the plectoneme. This results in the torsional energy of the system

$$E_T = 2\pi^2 \left(C(\lambda) \frac{Tw_\lambda^2}{(L_c - L_p)} + C(\bar{\lambda}) \frac{Tw_{\bar{\lambda}}^2}{L_p} \right) \tag{4.26}$$

where Tw_λ and $Tw_{\bar{\lambda}}$ are the twist values in the tails and in the plectoneme. The linking number density in plectoneme, $Tw_{\bar{\lambda}}$, and tails, Tw_λ, do not need to be the same. Twist relaxation is fast, as is confirmed by experiments [9]. Since the twist degree of freedom only couples globally, (by means of the White's equation), to the tangential degrees of freedom, we can integrate out the twist fluctuations and simplify the model by equating the twist free energy densities:

$$C(\lambda) \frac{Tw_\lambda^2}{(L_c - L_p)^2} = C(\bar{\lambda}) \frac{Tw_{\bar{\lambda}}^2}{L_p^2}. \tag{4.27}$$

We will use $Tw_\lambda/(L_c - L_p) \equiv tw_\lambda$ as one of the minimization parameters: $Tw_{\bar{\lambda}} \equiv tw_{\bar{\lambda}} L_p$ can be inferred from eq. (4.27). In principle, the end loop should be treated separately from the tails, with yet another λ. However the end loop only affects marginally the straight chain entropic contribution [34], justifying the use of a unique λ for tails and end loop. Therefore when writing Tw_λ and $Wr_{\text{loop}}(t)$ (see eq. (1.35)) we always mean the twist and the writhe of tails and loop together.

When using $Tw_\lambda/(L_c - L_p)$ as a minimization parameter, the length of the plectoneme L_p is given through White's relation eq. (1.38)

$$\begin{aligned} Lk &= (\text{Writhe} + \text{Twist})_{\text{plectoneme}} + (\text{Writhe} + \text{Twist})_{\text{tails}} \\ n &= (\omega(\alpha, t) + tw_{\bar{\lambda}}) L_p + Wr_{\text{loop}} + tw_\lambda (L_c - L_p) \end{aligned} \tag{4.28}$$

from which

$$L_p = \frac{n - Wr_{\text{loop}} - L_c tw_\lambda}{\omega(\alpha, t) + tw_{\bar{\lambda}} - tw_\lambda}. \tag{4.29}$$

Thermal fluctuations in the tails also modify, to lowest order, the $-fL_c$ term in equation (4.12) to

$$E_{\text{tails}} = \left(-f + \frac{k_B T}{\lambda} - \frac{(k_B T)^2}{4A}\right)(L_c - L_p) \tag{4.30}$$

and shorten the end-to-end distance by a factor $\rho_{\text{tail}} = 1 - \lambda k_B T/2A$ according to [47].

The total energy is thus

$$E_{\text{single}} = E_C + E_T + E_{\text{el}} + E_{\text{bend}} + E_{\text{loop}} + E_{\text{tails}} \tag{4.31}$$

4.5 Multi-plectoneme phase

From a purely mechanical point of view the energy cost of the end loop and tails is so high that only one plectoneme will form in the system, its length growing when increasing n. However the prominent role of thermal fluctuations and entropy could increase the contributions of multiple plectonemes, which act in this case as local minima. We call m the number of plectonemes, with total length L_p, given by equation (4.29) with $Wr_{\text{loop}} \to mWr_{\text{loop}}$. The total energy will be

$$E(m) = E_C + E_T + E_{\text{el}} + E_{\text{bend}} + mE_{\text{loop}} + E_{\text{tails}} \tag{4.32}$$

Assuming that L_p grows faster than m, we can neglect E_{loop} in eq. (4.32). This has the advantage that the minimization of the total energy with respect to $\alpha, R(t), \sigma_r$ and tw_λ is m-independent. The partition sum is computed with these values. We choose a hardcore repulsion between plectonemes (for simplicity) and a cutoff $\Lambda = 3.4$ nm (for structural reasons) to calculate[1] the density of states. The resulting partition sum is [21]

$$Z = e^{-E(0)} + \sum_{m=1} G_m e^{-E(m)} \tag{4.33}$$

$$G_m = \frac{\left(\rho_{\text{tail}}(L_c - L - p) - nL_{\text{loop}}\right)^n L_p^{n-1}}{n!\,(n-1)!\,\Lambda^n \Lambda^{n-1}} \tag{4.34}$$

[1]Removing the hardcore repulsion or changing the cutoff in a reasonable range affect the curves below the experimental error.

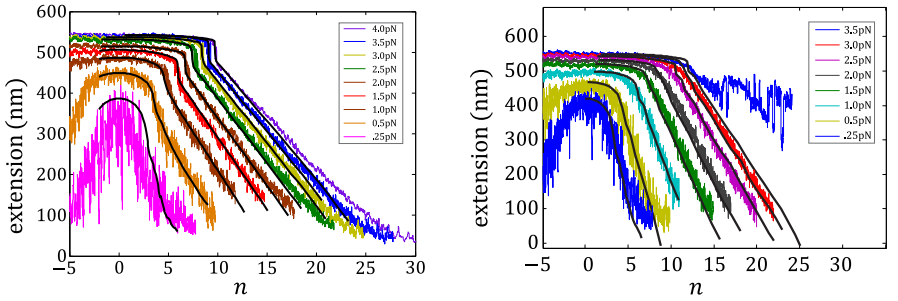

(a) 320 mM ionic strength. (b) 20 mM ionic strength.

Figure 4.3: Turns-extension plots comparison between the theory and experimental data from [5] for a DNA chain with contour length 600 nm.

where the upper limit is chosen so that $L_p \geq 0$. For long chains the distribution is strongly peaked around an average $\langle m \rangle$. There are 2 ways the extension decreases with increasing linking number, through an increase of plectoneme length and through an increase of the number of plectonemes. At high salt concentrations the single plectoneme configuration becomes the groundstate at finite plectoneme length. The jump as seen in experiments [24, 13] is partly caused by the end loop, partly by the finite size plectoneme. The nature of these configurations differs enough from the former to speak of a multi-plectoneme phase (MP): they affect the slope and the torque after the transition. To characterize the MP we introduce the multi-plectoneme parameter

$$\zeta \equiv \exp\left[-\frac{Wr_{\text{loop}}}{k_B T}\left(\frac{E_{\text{loop}}}{Wr_{\text{loop}}} - \frac{\Delta f}{\omega(\alpha,t)}\right)\right]\left(\frac{Wr_{\text{loop}}/L_{\text{loop}}}{\omega(\alpha,t)}\right)^2 \tag{4.35}$$

$$\Delta f = \frac{E_C + E_{\text{el}} + E_{\text{bend}}}{L_p} - \frac{E_{\text{tails}}}{L_c - L_p} \tag{4.36}$$

For $\zeta \ll 1$ the experimental turn-extension plots and torques, are well described by a single plectoneme whereas for $\zeta \approx 1$, the slope is a result of an increase of plectonemes with increasing n. The inset of Fig. 4.4a shows ζ as a function of salt concentration for different tensions.

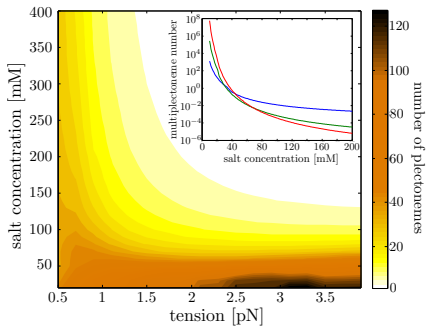

(a) Phase diagram of the average number of plectonemes as a function of tension and salt concentration for a 7.2 μm long chain. Note the shift of the maximum from low tension at high salt to high tension at low salt. The inset shows the MP parameter vs salt concentration for 1 pN (blue), 2 pN (green) and 3 pN (red).

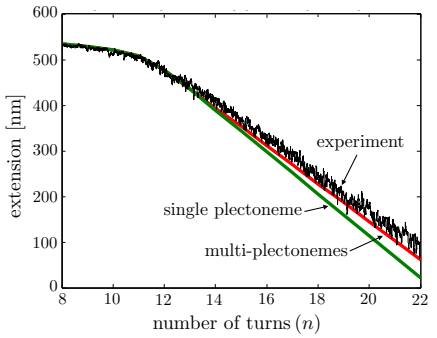

(b) The results of the theory with and without the possibility to form more than one plectoneme are presented alongside the experimental results (3 pN, 20 mM, experimental data from [5]).

Figure 4.4: How many plectonemes and do they make a difference?

4.6 Comparison to experiments

The predicted turn-extension plots of the model agree remarkably well with experiments, see Fig. 4.3. Our model has only two parameters, A and C, both known to some extent from other experiments. The general consensus for A is from 45 to 50nm k_BT. For the numerics we took $A = 50\text{nm}\, k_BT$+ OSF [52] corrections. The value of C influences foremost the transition point. To fit the measurements its value ranges from 100 to 120 nm k_BT. Only for a salt concentration of 20 mM, a lower value of 90 nm k_BT was needed to get the transition point right. Since the plectoneme length starts at 0 at the transition, our approximation of not treating the end loop separately is debatable. Detailed modelling of entropic and electrostatic repulsion within the end loop might improve the model, for example starting from [7], although in the end the proximity of the bifurcation point might invalidate a simple perturbation calculation. For low salt concentrations, older models predict slopes too step [5]. As

shown in Fig. 4.4b the MP phase corrects this picture.

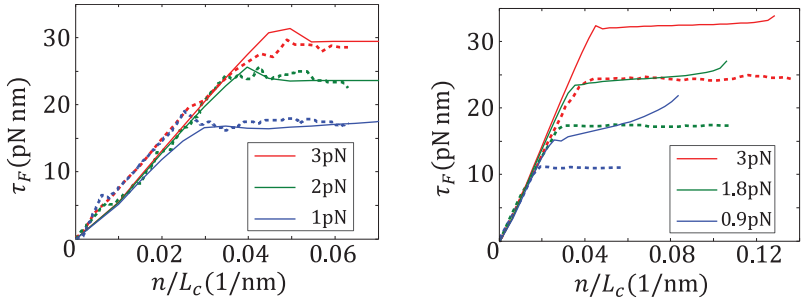

(a) 750 nm DNA chain at 150 mM ionic strength. Comparison between theory and torques directly measured [24].

(b) 5600 nm DNA chain at 100 mM ionic strength. Comparison between theory and inferred torques [48].

Figure 4.5: Predicted versus measured (dashed lines) torque.

In the MP phase the torque of the system is not constant after the transition. This could explain the difference between torques measured in optical tweezer experiments [24] and torques calculated using Maxwell relations in a magnetic tweezer setup [48]. The latter method assumes a constant torque after the transition. However, in the MP phase our theory predicts a non-constant torque. In Fig. 4.5b we show what our model predicts for the data presented in [48]. To facilitate comparison with the original paper, not the linking number, but the supercoiling density is used, defined as the ratio of the linking number density to the linking density of the two strands of free DNA. As can be seen in Fig. 4.5b, the assumption of constant torque underestimates the torque difference between the high and low tension curves. Our model, however, correctly reproduces the direct torque measurements of [24] (see figure 4.5a).

A final consequence of the MP phase is the change in the dynamics of plectonemes. Multiple plectonemes can change their length distribution fast as twist diffusion is fast [9]. This makes a fast diffusion of plectonemes possible also in the crowded environment of the plasmoid in bacteria or through a dense chromatin fiber in eukaryotes. The implications might be important, from cellular processes to transcription to segregation.